Journal of Dental Research
2016, Vol. 95(7) 742–751

DOI: 10.1177/0022034516640246
jdr.sagepub.com

Role of PHOSPHO1 in Periodontal Development and Function

L.E. Zweifler[1], M. Ao[2], M. Yadav[3], P. Kuss[3], S. Narisawa[3], T.N. Kolli[1], H.F. Wimer[4,5], C. Farquharson[6], M.J. Somerman[2], J.L. Millán[3], and B.L. Foster[1]

Abstract

The tooth root and periodontal apparatus, including the acellular and cellular cementum, periodontal ligament (PDL), and alveolar bone, are critical for tooth function. Cementum and bone mineralization is regulated by factors including enzymes and extracellular matrix proteins that promote or inhibit hydroxyapatite crystal growth. Orphan Phosphatase 1 (*Phospho1*, PHOSPHO1) is a phosphatase expressed by chondrocytes, osteoblasts, and odontoblasts that functions in skeletal and dentin mineralization by initiating deposition of hydroxyapatite inside membrane-limited matrix vesicles. The role of PHOSPHO1 in periodontal formation remains unknown and we aimed to determine its functional importance in these tissues. We hypothesized that the enzyme would regulate proper mineralization of the periodontal apparatus. Spatiotemporal expression of PHOSPHO1 was mapped during periodontal development, and *Phospho1*$^{-/-}$ mice were analyzed using histology, immunohistochemistry, in situ hybridization, radiography, and micro–computed tomography. The *Phospho1* gene and PHOSPHO1 protein were expressed by active alveolar bone osteoblasts and cementoblasts during cellular cementum formation. In *Phospho1*$^{-/-}$ mice, acellular cementum formation and mineralization were unaffected, whereas cellular cementum deposition increased although it displayed delayed mineralization and cementoid. *Phospho1*$^{-/-}$ mice featured disturbances in alveolar bone mineralization, shown by accumulation of unmineralized osteoid matrix and interglobular patterns of protein deposition. Parallel to other skeletal sites, deposition of mineral-regulating protein osteopontin (OPN) was increased in alveolar bone in *Phospho1*$^{-/-}$ mice. In contrast to the skeleton, genetic ablation of *Spp1*, the gene encoding OPN, did not ameliorate dentoalveolar defects in *Phospho1*$^{-/-}$ mice. Despite alveolar bone mineralization defects, periodontal attachment and function appeared undisturbed in *Phospho1*$^{-/-}$ mice, with normal PDL architecture and no evidence of bone loss over time. This study highlights the role of PHOSPHO1 in mineralization of alveolar bone and cellular cementum, further revealing that acellular cementum formation is not substantially regulated by PHOSPHO1 and likely does not rely on matrix vesicle–mediated initiation of mineralization.

Keywords: cementum, dentin, bone, periodontal ligament, extracellular matrix, physiologic calcification

Introduction

The periodontal apparatus, including acellular and cellular cementum, periodontal ligament (PDL), and alveolar bone, are critical for tooth attachment and function (Foster et al. 2007). Mineralization of dentin, cementum, and bone is regulated by several factors, including enzymes that modulate local inorganic phosphate (P_i) and pyrophosphate (PP_i) concentrations, and extracellular matrix (ECM) proteins that promote or inhibit hydroxyapatite crystal growth (Foster et al. 2012; Foster, Ao, et al. 2015). Although common mineralization regulators are expressed among these tissues, local differences in timing and expression levels provide tissue-specific regulatory mechanisms.

Orphan Phosphatase 1 (*Phospho1*, PHOSPHO1), a member of the haloacid dehalogenase superfamily of hydrolases, is expressed by chondrocytes, osteoblasts, and odontoblasts and has an indispensable role in skeletal mineralization. PHOSPHO1 is proposed to initiate deposition of crystalline hydroxyapatite inside cell-derived, membrane-limited matrix vesicles (MVs) by generating P_i from hydrolysis of MV membrane constituents, phosphoethanolamine and phosphocholine (Stewart et al. 2003, 2006; Houston et al. 2004; Roberts et al. 2007; Macrae et al. 2010; McKee et al. 2013). *Phospho1*$^{-/-}$ mice feature

[1]Division of Biosciences, College of Dentistry, Ohio State University, Columbus, OH, USA
[2]National Institute of Arthritis and Musculoskeletal and Skin Diseases, National Institutes of Health, Bethesda, MD, USA
[3]Sanford Children's Health Research Center, Sanford Burnham Prebys Medical Discovery Institute, La Jolla, CA, USA
[4]Department of Vertebrate Zoology, National Museum of Natural History, Smithsonian Institution, Washington, DC, USA
[5]National Institute of Dental and Craniofacial Research, National Institutes of Health, Bethesda, MD, USA
[6]Roslin Institute and Royal (Dick) School of Veterinary Studies, University of Edinburgh, Easter Bush, Midlothian, UK

A supplemental appendix to this article is published electronically only at http://jdr.sagepub.com/supplemental.

Corresponding Author:
B.L. Foster, Division of Biosciences, College of Dentistry, Ohio State University, 305 W. 12th Avenue, 4163 Postle Hall, Columbus, OH 43210, USA.
Email: foster.1004@osu.edu

scoliosis, osteomalacia, bowed long bones, and spontaneous fractures (Yadav et al. 2011; Rodriguez-Florez et al. 2015). The early role of PHOSPHO1 in mineralization is distinct from that of tissue nonspecific alkaline phosphatase (*Alpl;* TNAP), which reduces local concentrations of mineral inhibitor PP_i. Although individually knocking out either *Phospho1* or *Alpl* reduces skeletal mineralization, simultaneous ablation of both causes complete absence of mineralization in osteoblast cultures and developing embryos (Yadav et al. 2011; Huesa et al. 2015). *Phospho1*$^{-/-}$ mice also feature increased expression of ECM protein osteopontin (*Spp1*; OPN), contributing to inhibition of skeletal mineralization (Yadav et al. 2014).

Previously, we demonstrated that PHOSPHO1 is expressed by odontoblasts and functions in mineralization of mouse incisor dentin (McKee et al. 2013). However, the role of PHOSPHO1 in periodontogenesis remains unknown, and we aimed to determine its importance in formation and function of the periodontium. We mapped spatiotemporal expression of PHOSPHO1, analyzed postnatal tooth development in *Phospho1*$^{-/-}$ mice, and evaluated the potential pathological role for increased OPN in the dentition of *Phospho1*$^{-/-}$ mice.

Materials and Methods

Animals

Animal procedures were performed in accordance with guidelines of the Animal Care and Use Committee at the Sanford Burnham Prebys Medical Discovery Institute and National Institutes of Health (NIH). To detect *Phospho1* mRNA and protein expression during tooth development, tissues were collected from C57BL/6 mice at 4, 5, 14, 15, and 26 d postnatal (dpn) (n = 3 to 5 per group). *Phospho1*$^{-/-}$ mice (Yadav et al. 2011) and *Spp1*$^{-/-}$ mice (Rittling et al. 1998) have been described previously. Details on breeding and genotyping are found in the Appendix. For analysis of wild-type (WT), *Phospho1*$^{-/-}$, *Spp1*$^{-/-}$, and *Phospho1*$^{-/-}$; *Spp1*$^{-/-}$ mice, mandibles were collected at 14 dpn (n = 3), 30 dpn (n = 3 to 12), and 90 dpn (n = 2 to 6).

Radiography and Micro–Computed Tomography

Hemi-mandibles were scanned in a cabinet X-ray (Faxitron X-ray Corp.) at 30 kV for 40 s. For micro–computed tomography (micro-CT), formalin-fixed mandibles were scanned on a Scanco Medical micro-CT 50 (Scanco Medical AG) with parameters of 9 µm voxel size, 55 KVp, and 145 mA, with a 0.36° rotation step (180° angular range) and a 400-ms exposure per view. Exported DICOM files were reoriented using ImageJ software (1.48r; NIH) to compare coronal and sagittal planes of sections. DICOM stacks were rendered as 3-dimensional (3D) isoimages using Amira software (version 6.0; FEI). Quantitative micro-CT analysis was performed as described previously (Foster, Sheen, et al. 2015), and details are provided in the Appendix. Tissue volume (TV), bone volume (BV), bone volume fraction (BV/TV), bone thickness, and tissue mineral density (TMD) were calculated.

Histology

Mandibles fixed in 10% neutral buffered formalin were prepared for histology by decalcifying in 10% (v/v) glacial acetic acid, 4% (v/v) neutral buffered formalin, and 0.85% (w/v) sodium chloride and embedding in paraffin prior to making 6-µm serial sections. Sections underwent hematoxylin and eosin (H&E) staining (Foster 2012). Histomorphometry was performed on H&E-stained sections using a slide scanner (Leica SCN400F) with Digital Imaging Hub software (Leica Microsystems). Details on measurements are provided in the Appendix. To evaluate collagen fiber organization, sections were stained by picrosirius red (Polysciences, Inc.) as described previously (Foster 2012). Non-decalcified 30 dpn hemi-mandibles were embedded in methyl methacrylate for von Kossa and Goldner's trichrome staining, as described previously (Foster et al. 2013).

Immunohistochemistry and In Situ Hybridization

In situ hybridization (ISH) with a digoxigenin-labeled antisense *Phospho1* cRNA probe was performed on paraffin-embedded sections as previously described (Kuss et al. 2009), with indoxyl-nitroblue tetrazolium substrate to produce a blue reaction. ISH with an antisense *Spp1* probe was performed on paraffin-embedded sections and visualized with fast red dye (Advanced Cell Diagnostics), using hematoxylin as a counterstain.

Immunohistochemistry (IHC) was performed on paraffin-embedded sections using an avidin-biotinylated peroxidase enzyme complex–based kit (Vector Labs) with a 3-amino-9-ethylcarbazole substrate (Vector Labs) to produce a red reaction (Foster 2012). Hematoxylin was used as the counterstain. Primary antibodies included monoclonal rat IgG anti-human TNAP (R&D Systems) (Zweifler et al. 2015), polyclonal rabbit anti-mouse bone sialoprotein (BSP) (Dr. Renny Franceschi, University of Michigan, Ann Arbor) (Foster 2012), polyclonal LF-175 rabbit anti-mouse OPN (Dr. Larry Fisher, National Institute for Dental and Craniofacial Research) (Foster 2012), and human recombinant Fab monoclonal anti-PHOSPHO1 (AbD Serotec, MorphosysAG) (McKee et al. 2013).

Quantitative Polymerase Chain Reaction

RNA was isolated from long bones (femurs), calvaria, molars, and brain tissues of WT mice at 15 dpn for gene expression analysis. For periodontal tissue mRNA analysis, first mandibular molars were extracted at 5, 14, and 26 dpn (excluding gingiva and bone) and RNA was harvested from attached tissues using a purification kit (RNeasy; Qiagen). cDNA was synthesized to perform quantitative polymerase chain reaction (qPCR) (Lightcycler 2.0; Roche Applied Science). Primers used to amplify *Phospho1* (NM_153104.3) transcripts in bones and teeth were as follows: GGGTGGATAAGACCGCGTA (forward) and CTTAACCACC ACCTTTAGAAACTGT (reverse). Primers used for qPCR of PDL tissues were proprietary sequences included in a polymerase chain reaction array (Qiagen).

Statistical Analysis

Mean values were compared by 1-way analysis of variance or independent-samples *t* tests using GraphPad Prism 6.01 software.

Results

PHOSPHO1 Is Expressed during Tooth Root and Periodontal Development

Just prior to molar root formation at 5 dpn, *Phospho1*/PHOSPHO1 was expressed at high levels in newly differentiated odontoblasts (Fig. 1A, B). During molar root formation, PHOSPHO1 was localized to regions of alveolar bone remodeling (e.g., the crest), and new root odontoblasts maintained expression, albeit at relatively reduced levels (Fig. 1C–F). Minimal *Phospho1* mRNA was detected in the follicle near forming acellular cementum, and PHOSPHO1 protein was undetectable. At completion of root formation, odontoblasts no longer expressed PHOSPHO1 (data not shown); however, mRNA and protein were found in regions of cellular cementum formation (Fig. 1G, H). qPCR data from mouse tissues indicated that, like long bone and calvarial bone, molars expressed *Phospho1* mRNA (Fig. 1I), likely in odontoblasts. qPCR performed on RNA isolated from PDL tissues confirmed ISH and IHC findings, showing significantly increasing *Phospho1* expression during root formation, at 14 and 26 dpn (Fig. 1J). Although ameloblasts showed positive PHOSPHO1 protein localization (Fig. 1A, B), no mRNA could be detected by ISH in the enamel organ.

Mineralization of Cellular but Not Acellular Cementum Is Dependent on PHOSPHO1

Because PHOSPHO1 functions in bone and dentin mineralization, we suspected it to perform a similar function in cementum. Acellular cementum is the first type of cementum formed and covers the cervical portions of molar roots. Examination of mandibular first molars in *Phospho1*$^{-/-}$ mice and WT controls at 14, 30, and 90 dpn revealed no apparent deficiency in acellular cementum growth (Fig. 2A–F). Histomorphometry confirmed no decrease and, in fact, indicated a trend of increased width in acellular cementum of *Phospho1*$^{-/-}$ mouse molars compared with WT controls (Fig. 2G, H). OPN immunostaining revealed no delay in acellular cementum initiation in *Phospho1*$^{-/-}$ versus WT molars (Fig. 2A, B insets, I). Goldner's trichrome staining performed on undecalcified 30-dpn samples revealed a mineralized acellular cementum layer on the surface of *Phospho1*$^{-/-}$ molar roots, similar in appearance to WT cementum (Fig. 2C, D insets).

Cellular cementum is deposited on the apical portions of molar teeth. Analysis of mandibular first molars in *Phospho1*$^{-/-}$ mice and WT controls at 30 and 90 dpn revealed increased deposition of cellular cementum (Fig. 3A–H). Histomorphometry confirmed a statistically significant increase in cellular cementum area in *Phospho1*$^{-/-}$ compared with WT molars at 30 dpn and a similar trend at 90 dpn (Fig. 3I). By H&E staining, *Phospho1*$^{-/-}$ cellular cementum showed apparent mineralization delays and 20- to 30-μm cementoid accumulation at the surface (yellow dotted outlines and arrows in Fig. 3D, H), and Goldner's trichrome staining of undecalcified sections confirmed this as cementoid (Fig. 3B, D, insets).

Although the function of PHOSPHO1 in incisor dentin at early postnatal ages has been previously examined (McKee et al. 2013), its role in molar formation has not yet been studied. Because both acellular and cellular cementum form on the surface of dentin, in cementum and periodontal analysis, it is important to understand the status of the underlying dentin. Using radiography, micro-CT, histology, and IHC, we confirmed the importance of PHOSPHO1 in both molar and incisor root dentin, based on delayed dentin mineralization and an abnormal and expanded mantle dentin in *Phospho1*$^{-/-}$ compared with WT mice (Appendix Figs. 2–4).

Alveolar Bone Mineralization and Periodontal Function in the Absence of PHOSPHO1

Alveolar bone of *Phospho1*$^{-/-}$ mice at early postnatal ages was hypomineralized with accumulation of osteoid on the bone surface (McKee et al. 2013). We wondered whether this defect was limited to early ages or extended into adulthood with potential effects on periodontal function. By H&E staining, alveolar bone of *Phospho1*$^{-/-}$ mice showed apparent mineralization delays and 20- to 30-μm or more osteoid accumulation at the alveolar bone crest (ABC), even at 90 dpn (Fig. 4A–D). The mineralization front in *Phospho1*$^{-/-}$ alveolar bone exhibited a globular pattern (Fig. 4A, C, insets), suggesting inhibition of mineralization. Von Kossa staining of undecalcified samples at 30 dpn confirmed the mineralization delay and globular patterning in alveolar bone of *Phospho1*$^{-/-}$ compared with WT mice (Fig. 4E–H). IHC for BSP, a mineral-binding ECM protein, revealed a similar globular deposition pattern in alveolar bone of *Phospho1*$^{-/-}$ mice (Fig. 4I, K). IHC additionally revealed increased OPN localization in alveolar bone of *Phospho1*$^{-/-}$ mice compared with the WT (Fig. 4J, L); however, ISH did not indicate increased *Spp1* mRNA in dentoalveolar tissue (Fig. 4J, L, insets). Quantitative micro-CT analysis revealed a statistically significant 10% reduction in BV/TV, and a nonsignificant trend of decreased TMD in alveolar bone of *Phospho1*$^{-/-}$ mice compared with WT (Fig. 4M, N). Micro-CT data for all dental tissues are summarized in the Appendix Table.

Increased levels of OPN contribute to the pathological skeletal hypomineralization in *Phospho1*$^{-/-}$ mice (Yadav et al. 2014), prompting us to determine whether genetic ablation of OPN would ameliorate defects in *Phospho1*$^{-/-}$ alveolar bone. Histology and micro-CT analysis of *Phospho1*$^{-/-}$; *Spp1*$^{-/-}$ mice showed no qualitative or quantitative improvement in alveolar bone mineralization compared with *Phospho1*$^{-/-}$ mice (Appendix Fig. 5, Appendix Table). Defects in *Phospho1*$^{-/-}$ molar and incisor dentin were similarly not ameliorated by ablation of *Spp1* (Appendix Fig. 6).

Based on alterations in alveolar bone and cellular cementum mineralization in *Phospho1*$^{-/-}$ mice, we asked whether

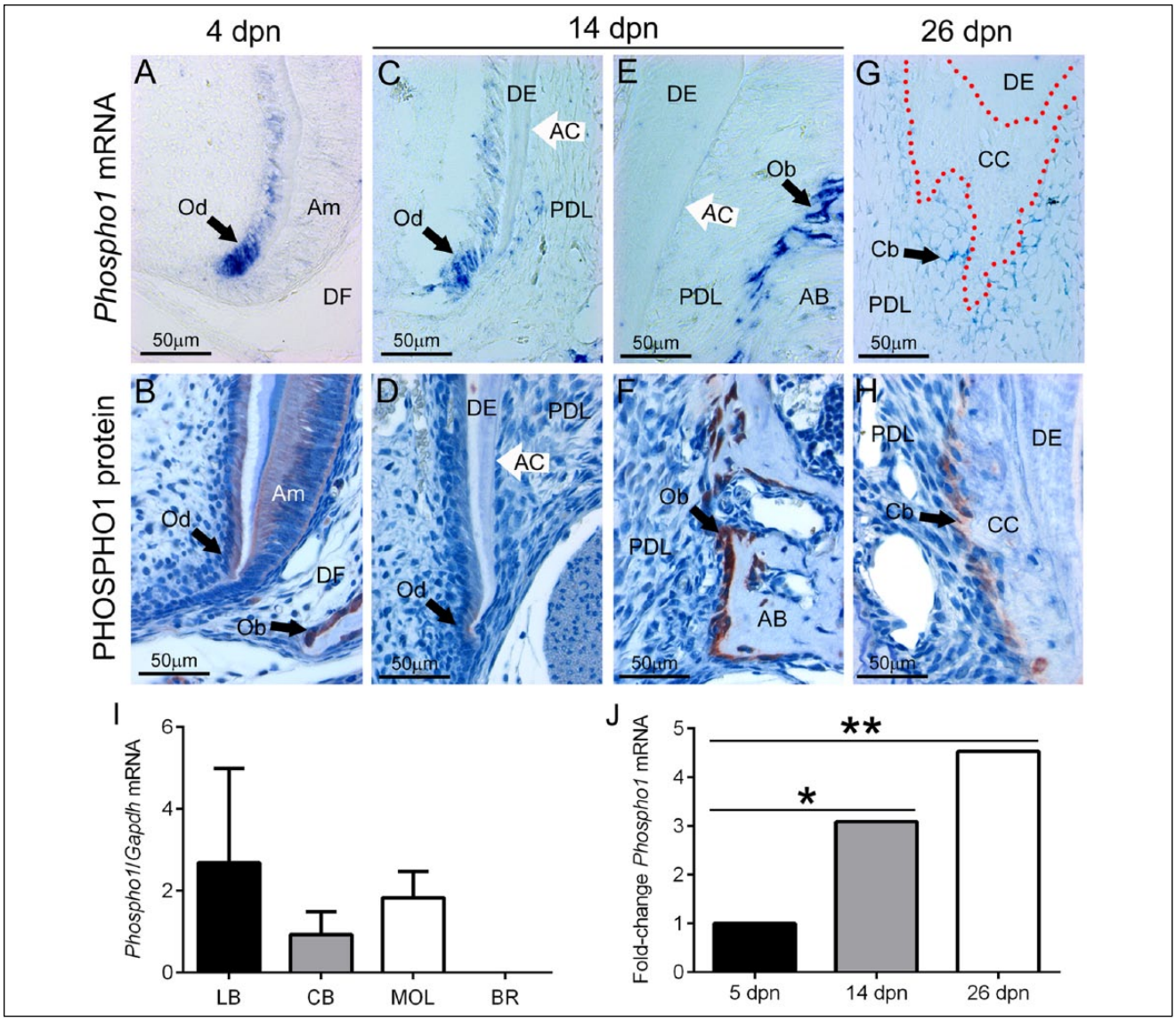

Figure 1. PHOSPHO1 is expressed in periodontal tissues during development. During tooth root and periodontal development, *Phospho1* mRNA was localized by in situ hybridization (ISH; top row) and PHOSPHO1 protein was localized by immunohistochemistry (IHC; second row). (**A, B**) Just prior to initiation of root formation at 4 d postnatal (dpn), ISH and IHC staining of *Phospho1*/PHOSPHO1 shows elevated expression in osteoblasts (Ob) of actively forming alveolar bone (AB) and in newly differentiated odontoblasts (Od) in the first molar tooth. Ameloblasts (Am) show positive IHC staining, but no ISH signal. DF, dental follicle. (**C, D**) During root formation at 14 dpn, highest PHOSPHO1 is localized to regions of AB modeling, with weaker expression in new odontoblasts forming root dentin (DE). Weak mRNA and no protein is detected in apical regions near new acellular cementum (AC). (**E, F**) Neither mRNA nor protein is found near AC on the cervical region of the root. (**G, H**) Cementoblasts (Cb) associated with cellular cementum (CC) formation showed positive staining for both *Phospho1* mRNA and PHOSPHO1 protein. (**I**) *Phospho1* mRNA is detected in mouse long bone (LB), calvarial bone (CB), and molars (MOL) at 15 dpn, although expression in brain (BR) is negligible ($n = 3$ for each). (**J**) Quantitative polymerase chain reaction performed on RNA isolated from mouse PDL tissues ($n = 3$) confirms that *Phospho1* expression is detected during root formation at 5, 14, and 26 dpn, with increased expression over time (*$P < 0.05$; **$P < 0.01$, compared with expression at 5 dpn).

periodontal function was maintained over time. Picrosirius red staining observed under polarized light indicated apparently normal collagen attachment and organization in 30 and 90 dpn *Phospho1*$^{-/-}$ mice (Fig. 5A–D). Both 2-dimensional and 3D micro-CT analysis did not identify obvious alveolar bone loss surrounding *Phospho1*$^{-/-}$ mandibular molars (Fig. 5E–J shows 90-dpn samples, Appendix Fig. 7 shows 30-dpn samples). Histomorphometry indicated no signs of vertical or horizontal bone loss (cementoenamel junction [CEJ]–ABC distance and alveolar bone width) and indicated no significant changes in PDL width (Fig. 5K, L).

Discussion

PHOSPHO1 is a phosphatase that functions in skeletal and dental mineralization by initiating deposition of hydroxyapatite within the lumen of MVs (Stewart et al. 2003; Houston et al. 2004; Roberts et al. 2007; Macrae et al. 2010; McKee et al.

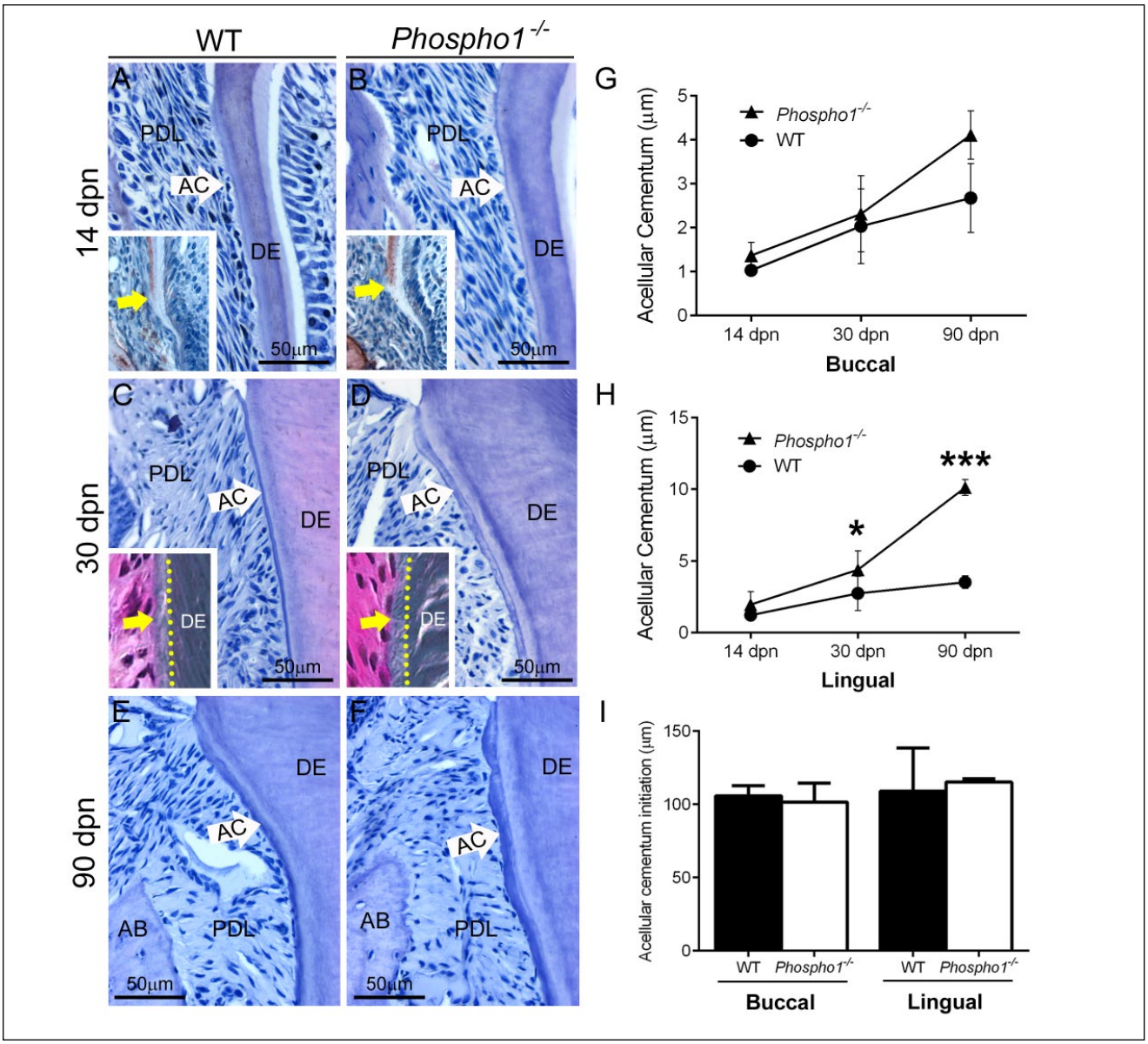

Figure 2. Acellular cementum is not defective in *Phospho1*$^{-/-}$ mice. (**A–F**) Observation and histomorphometry of hematoxylin and eosin–stained histological sections of the first mandibular molar at 14, 30, and 90 d postnatal (dpn) reveals no defect in acellular cementum (AC) in *Phospho1*$^{-/-}$ compared with wild-type (WT) mice. (**G, H**) Histomorphometry of AC width indicates no deficit in *Phospho1*$^{-/-}$ mice compared with controls and a trend for increased AC thickness (*$P < 0.05$; ***$P < 0.001$). Osteopontin (OPN) immunostaining (insets in A, B) indicates no delay in AC initiation in *Phospho1*$^{-/-}$ versus WT molars at 14 dpn, confirmed by histomorphometric measurement in (**I**). Goldner's trichrome staining (insets in C, D) performed on 30 dpn undecalcified samples suggests a similarly mineralized AC layer on *Phospho1*$^{-/-}$ and WT molar roots. Dentin (DE) defects are described in Appendix Figures 2 to 4. AB, alveolar bone; PDL, periodontal ligament.

2013). Here, we show that PHOSPHO1 is expressed by alveolar bone osteoblasts and cementoblasts during cellular cementum formation. In the absence of PHOSPHO1, mineralization defects were found in alveolar bone and cellular cementum, although acellular cementum was unaffected by loss of PHOSPHO1, and periodontal attachment and function appeared undisturbed. In parallel to skeletal sites (Yadav et al. 2014), OPN deposition, although not mRNA expression, was increased in alveolar bone of *Phospho1*$^{-/-}$ mice. In contrast with the skeleton, ablation of *Spp1* did not ameliorate defects in *Phospho1*$^{-/-}$ dentoalveolar tissues. Although this study highlights a role for PHOSPHO1 in the mineralization of periodontal tissues, the loss of PHOSPHO1 does not severely affect periodontal function.

PHOSPHO1 Functions in Alveolar Bone Mineralization

Previous studies have shown *Phospho1* gene and PHOSPHO1 protein expression in chondrocytes and osteoblasts of the postcranial skeleton and craniofacial region (Houston et al. 2004;

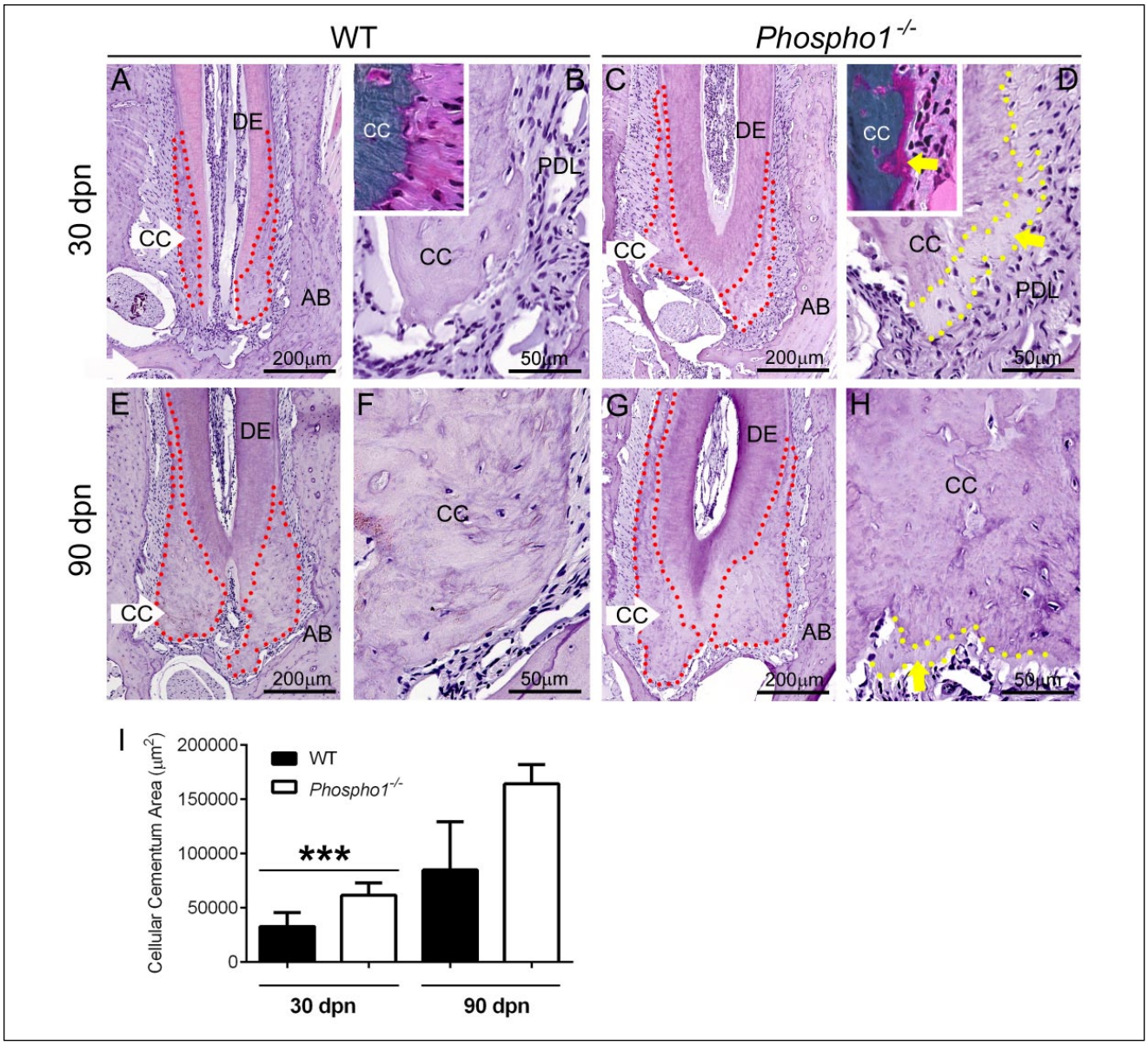

Figure 3. Cellular cementum mineralization is delayed in *Phospho1*$^{-/-}$ mice. (**A, C, E, G, I**) Observation and histomorphometry of hematoxylin and eosin–stained histological sections of the first mandibular molar at 30 and 90 d postnatal (dpn) reveals a trend of increased cellular cementum (CC) deposition in *Phospho1*$^{-/-}$ compared with wild-type (WT) mice (***$P < 0.001$ at 30 dpn). The CC perimeter is indicated by red dotted outlines in A, C, E, and G. (**B, D, F, H**) *Phospho1*$^{-/-}$ CC shows apparent mineralization delays and 20- to 30-μm cementoid accumulation at the surface (dotted yellow outlines and yellow arrows in D and H), and Goldner's trichrome staining of undecalcified mandible sections at 30 dpn confirms this unmineralized cementoid accumulation (insets in B, D). AB, alveolar bone; DE, dentin; PDL, periodontal ligament.

Stewart et al. 2006; Roberts et al. 2007). Inhibition of PHOSPHO1 activity in chick limbs or genetic ablation of *Phospho1* in mice results in impaired mineralization, confirming a critical and nonredundant role in skeletal development (Macrae et al. 2010; Huesa et al. 2011; Yadav et al. 2011). *Phospho1*$^{-/-}$ mice feature reduced body size, short femurs and tibias, osteomalacia, bowed long bones, increased bone fractures, and scoliosis (Yadav et al. 2011). PHOSPHO1 protein is also expressed in odontoblasts at early postnatal ages, and genetic ablation of *Phospho1* in mice causes delayed dentin mineralization (McKee et al. 2013).

Here, we report that PHOSPHO1 is detected in osteoblasts coincident with intramembranous ossification associated with new alveolar bone formation and postnatal remodeling, even into adulthood. In parallel to findings in the postcranial skeleton, *Phospho1*$^{-/-}$ mice exhibited delayed alveolar bone mineralization, accumulation of osteoid, abnormal deposition of ECM proteins indicative of mineralization defects, and significantly reduced BV/TV compared with WT mice. A previous study revealed that PHOSPHO1 regulated the mechanical properties of tibial bone in an age-dependent manner, with partial correction of bone ductile properties at advanced ages (Javaheri et al.

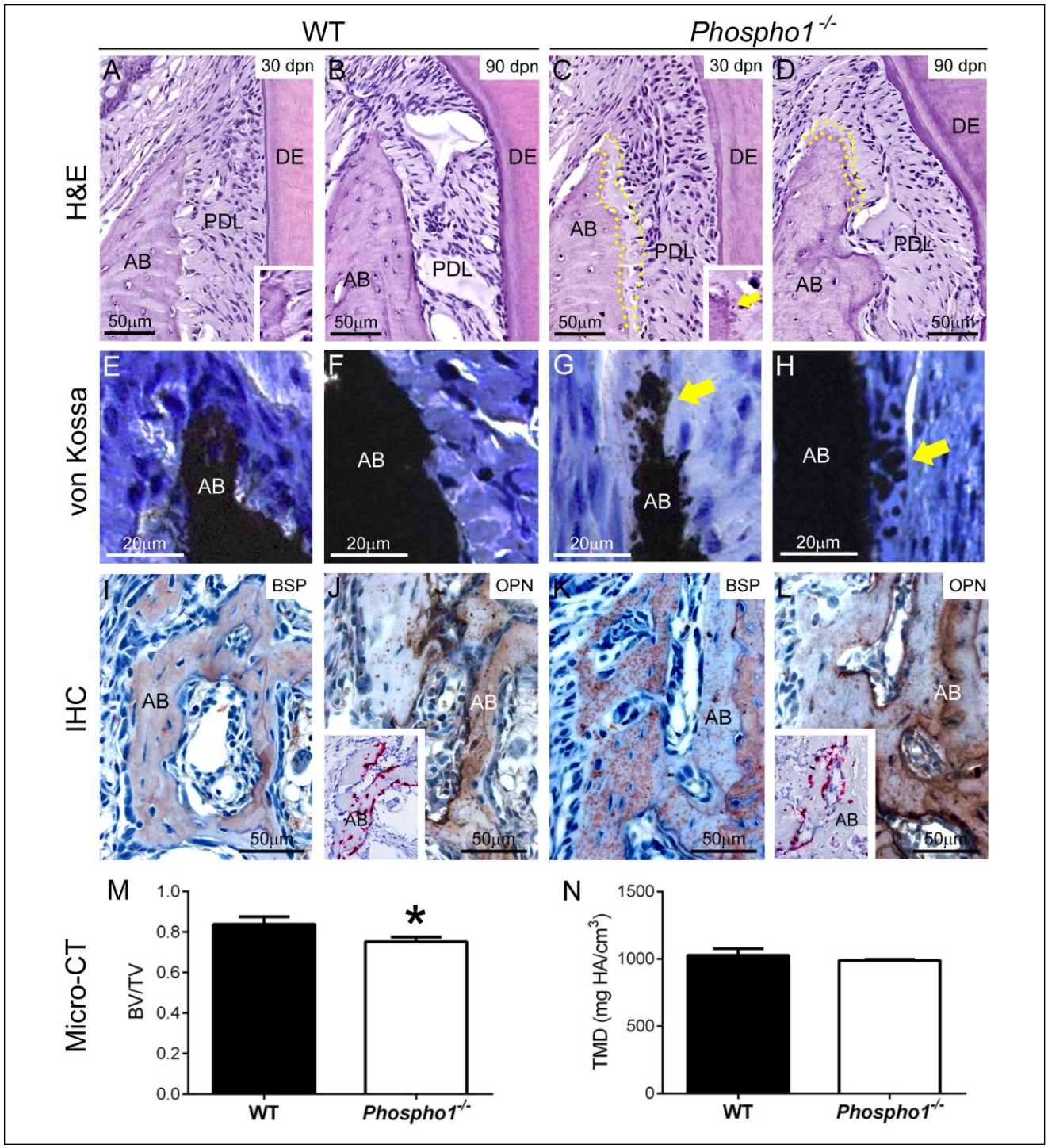

Figure 4. Persistent alveolar bone defects in *Phospho1*$^{-/-}$ mice. (**A–D**) Observation of hematoxylin and eosin–stained histological sections of first mandibular molar regions at 30 and 90 d postnatal (dpn) reveals apparent mineralization delays and 20 to 30 μm of osteoid accumulation at the alveolar bone (AB) crest (indicated by yellow dotted outlines) of *Phospho1*$^{-/-}$ mice compared with controls. The mineralization front in *Phospho1*$^{-/-}$ mouse AB appears globular, indicative of inhibition of mineralization (insets in A, C, yellow arrow in C). (**E–H**) Von Kossa staining of undecalcified samples at 30 dpn confirmed globular mineralization defects (yellow arrows) in *Phospho1*$^{-/-}$ AB compared with the wild type (WT). (**I, K**) Immunostaining for bone sialoprotein (BSP) reveals a globular deposition pattern in AB of *Phospho1*$^{-/-}$ mice compared with WT mice. (**J, L**) Immunostaining for osteopontin (OPN) reveals increased localization in AB of *Phospho1*$^{-/-}$ mice compared with WT mice. Inserts in J and L show that in situ hybridization does not indicate increased *Spp1* mRNA expression in alveolar bone of *Phospho1*$^{-/-}$ mice. (**M, N**) Quantitative micro–computed tomography (micro-CT) analysis reveals a statistically significant 10% reduction in BV/TV (M) and a nonsignificant trend of decreased TMD in AB (N) of *Phospho1*$^{-/-}$ mice compared with WT mice. Micro-CT data for all dental tissues are summarized in the Appendix Table. DE, dentin; IHC, immunohistochemistry; PDL, periodontal ligament.

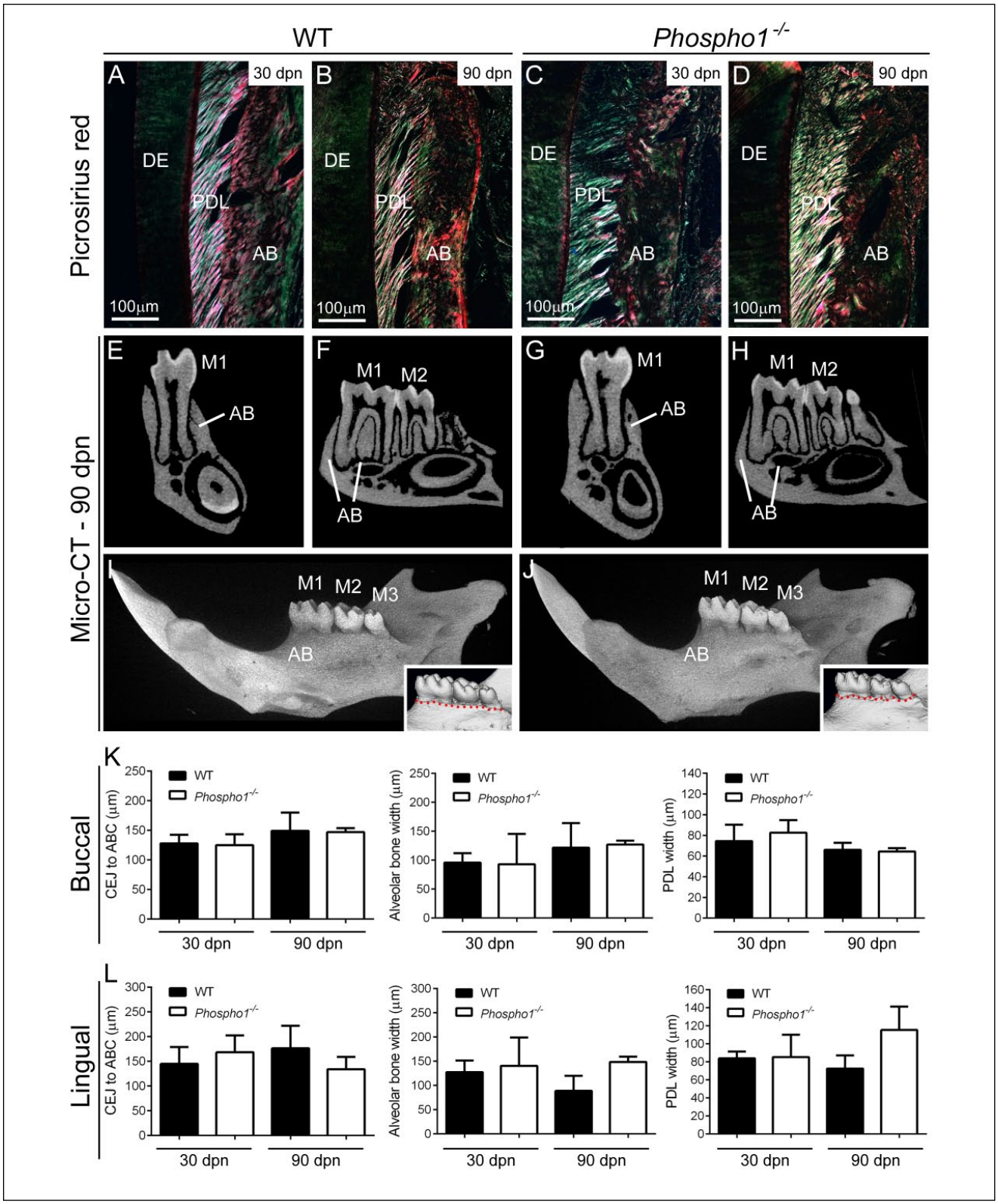

Figure 5. Loss of PHOSPHO1 does not inhibit periodontal function. (**A–D**) Observation of picrosirius red stained 30- and 90-dpn tissues under polarized light indicated similar collagen attachment to teeth and alveolar bone (AB), and periodontal ligament (PDL) organization in *Phospho1*$^{-/-}$ and wild-type (WT) control mice. (**E–J**) Analysis of micro–computed tomography (micro-CT) 2-dimensional cross-sections and 3-dimensional renderings at 90 dpn does not indicate AB loss surrounding the mandibular molars (M1, M2, and M3). Insets in I and J show similar alveolar crest height (red dotted line) in *Phospho1*$^{-/-}$ and WT mice. Micro-CT results from 30-dpn samples are shown in Appendix Figure 7. (**K, L**) Histomorphometry confirms similar cementoenamel junction (CEJ)–alveolar bone crest (ABC) distance, AB width, and PDL width, on buccal and lingual aspects of mandibular M1 in *Phospho1*$^{-/-}$ mice compared with controls ($P > 0.05$ in independent-samples *t* test). DE, dentin.

2015). Although consistent bulk mineralization defects were apparent in alveolar bone, the alveolar crest appeared most dramatically affected, with persistent osteoid accumulation. This is consistent with the role of PHOSPHO1 in initiation of mineralization and reports that alveolar bone is among the most rapidly remodeling bone (Beertsen et al. 1997). The alveolar crest, in particular, is continually remodeled in response to mechanical loading of teeth, and we have previously identified mineralization defects at this site in other mouse models of hypomineralization (Foster et al. 2013; Foster, Sheen, et al. 2015; Zweifler et al. 2015). The continuing importance of PHOSPHO1 in alveolar bone mineralization identifies this protein as a potential factor of interest in ongoing periodontal function and regeneration.

OPN is an ECM protein and member of the Small Integrin Binding Ligand N-Linked Glycoprotein (SIBLING) family (Fisher and Fedarko 2003) capable of functioning as a negative regulator of physiological and pathological mineralization (Jono et al. 2000; Boskey 2002; Yuan et al. 2014). Increased expression and deposition of OPN in the skeleton and increased circulating OPN protein were shown to contribute to the skeletal pathology in *Phospho1*$^{-/-}$ mice (Yadav et al. 2014). In parallel to other skeletal sites, we detected increased deposition of OPN in alveolar bone of *Phospho1*$^{-/-}$ mice, although there was no evidence of locally increased *Spp1* mRNA by ISH, and qPCR analysis was not performed. These data point toward increased circulating OPN protein as the source for increased deposition in dentoalveolar tissues (VandenBos et al. 1999). In contrast with findings that genetic ablation of *Spp1* partially corrected skeletal mineralization defects, we found no qualitative or quantitative evidence that OPN deficiency ameliorated alveolar bone (or dentin) defects in *Phospho1*$^{-/-}$ mice. This suggests that OPN does not play a significant role in the pathological hypomineralization of *Phospho1*$^{-/-}$ dentoalveolar tissues, prompting questions about whether OPN functions differently at different dental/skeletal sites, and whether and how OPN modulates or is modulated by other mineralization regulators that may confer tissue-specific differences. This underlines the need for further studies on the role of OPN in dentoalveolar development.

A Role for PHOSPHO1 in Cementogenesis

We found no discernible effect of *Phospho1* knockout on acellular cementum development or function, although cellular cementum exhibited delayed mineralization similar to bone. There is a striking correlation between the mineralization defects in *Phospho1*$^{-/-}$ mice and the known distribution of MVs, which have been found in alveolar bone, dentin, and cellular cementum but have not been identified in acellular cementum formation (Takano et al. 2000). These observations agree with the known functional importance of PHOSPHO1 in MV-initiated hydroxyapatite mineralization. However, the lack of an acellular cementum phenotype is striking in another sense; acellular cementum was found to be the most sensitive of dentoalveolar tissues to disturbances of mineralization caused by a number of other factors (Foster et al. 2011; Foster et al. 2012; Foster et al. 2013; Foster, Ao, et al. 2015; Zweifler et al. 2015) but here is resistant to loss of PHOSPHO1. Mouse models with defective cementum and/or alveolar bone attachment owing to genetic defects (e.g., *Alpl*$^{-/-}$, *Bsp*$^{-/-}$, and *Dmp1*$^{-/-}$ mice) feature detachment and disorganization of the PDL, widespread osteoclastic destruction of alveolar bone, and a breakdown of periodontal function akin to periodontal disease in humans, in the range of 1 to 2 months of age (Ye et al. 2008; Foster et al. 2013; Foster, Ao, et al. 2015; Gasque et al. 2015; Soenjaya et al. 2015; Zweifler et al. 2015). Although *Phospho1*$^{-/-}$ mice exhibit defective alveolar bone mineralization, no significant periodontal destruction is evident, further confirming that acellular cementum is functional, as is the periodontal complex.

Cellular cementum responded similarly to bone in *Phospho1*$^{-/-}$ mice, exhibiting hypomineralization, cementoid accumulation, and altered morphology, in this case, significantly increased deposition. Although the proximal cause for increased cellular cementum deposition in *Phospho1*$^{-/-}$ mice remains elusive, 2 possible mechanisms present themselves. First, alterations in underlying dentin may induce changes in cellular cementum. As we observed previously (McKee et al. 2013) and confirmed and extended in this study, effects of PHOSPHO1 deficiency manifest primarily in the outermost mantle dentin layer that serves as the substrate for cellular cementum deposition. A second mechanism for increased cellular cementum may be compensation resulting from disturbed synthesis and/or compromised mechanical properties. In support of this theory, a very similar increase in hypomineralized cellular cementum has been found when mineralization is disturbed in *Alpl*$^{-/-}$ mice (Zweifler et al. 2015) and in mice treated with 1-hydroxyethylidene-1,1-bisphosphonate (Takano et al. 2003). Divergent effects of loss of PHOSPHO1 on acellular versus cellular cementum further underscore developmental and regulatory differences between these tissues.

Author Contributions

L.E. Zweifler, contributed to data acquisition, analysis, and interpretation, drafted and critically revised the manuscript; M. Ao, P. Kuss, T.N. Kolli, H.F. Wimer, contributed to data acquisition, analysis, and interpretation, critically revised the manuscript; M. Yadav, contributed to design, data acquisition, analysis, and interpretation, critically revised the manuscript; S. Narisawa, contributed to conception, design, data acquisition, analysis, and interpretation, critically revised the manuscript; C. Farquharson, M.J. Somerman, contributed to conception and design, critically revised the manuscript; J.L. Millán, contributed to conception, design, data analysis, and interpretation, critically revised the manuscript; B.L. Foster, contributed to conception, design, data acquisition, analysis, and interpretation, drafted and critically revised the manuscript. All authors gave final approval and agree to be accountable for all aspects of the work.

Acknowledgments

This research was supported by grants from the National Institutes of Health (NIH) National Institute for Dental and Craniofacial Research (NIDCR) (DE12889 to J.L.M.), the Biotechnology and Biological Sciences Research Council (BB/J004316/1 to C.F.), the

NIH National Institute of Arthritis and Musculoskeletal and Skin Diseases (NIAMS) (AR53102 to J.L.M. and AR066110 to B.L.F.), and the Intramural Research Program of NIAMS (to M.J.S.), as well as by a Dr. Rudy Melfi Fellowship from the Ohio State University College of Dentistry (to L.E.Z.). The authors thank Nasrin Kalantari Pour (NIAMS/NIH) for histology, Anne Tran and Alyssa Coulter (NIAMS/NIH) for assistance with immunostaining, Kristina Zaal (NIAMS Light Imaging Section) for assistance with slide scanning, Kenn Holmbeck (NIDCR/NIH) for assistance with micro-CT scanning, and Lyudmila Lukashova (Hospital for Special Surgery) for assistance with micro-CT analysis. The authors declare no potential conflicts of interest with respect to the authorship and/or publication of this article.

References

Beertsen W, McCulloch CA, Sodek J. 1997. The periodontal ligament: a unique, multifunctional connective tissue. Periodontol 2000. 13:20–40.

Boskey AL. 2002. Variations in bone mineral properties with age and disease. J Musculoskelet Neuronal Interact. 2(6):532–534.

Fisher LW, Fedarko NS. 2003. Six genes expressed in bones and teeth encode the current members of the sibling family of proteins. Connect Tissue Res. 44(Suppl 1):33–40.

Foster BL. 2012. Methods for studying tooth root cementum by light microscopy. Int J Oral Sci. 4(3):119–128.

Foster BL, Ao M, Willoughby C, Soenjaya Y, Holm E, Lukashova L, Tran AB, Wimer HF, Zerfas PM, Nociti FH Jr, et al. 2015. Mineralization defects in cementum and craniofacial bone from loss of bone sialoprotein. Bone. 78:150–164.

Foster BL, Nagatomo KJ, Bamashmous SO, Tompkins KA, Fong H, Dunn D, Chu EY, Guenther C, Kingsley DM, Rutherford RB, et al. 2011. The progressive ankylosis protein regulates cementum apposition and extracellular matrix composition. Cells Tissues Organs. 194(5):382–405.

Foster BL, Nagatomo KJ, Nociti FH, Fong H, Dunn D, Tran AB, Wang W, Narisawa S, Millán JL, Somerman MJ. 2012. Central role of pyrophosphate in acellular cementum formation. PLoS One. 7(6):e38393.

Foster BL, Popowics TE, Fong HK, Somerman MJ. 2007. Advances in defining regulators of cementum development and periodontal regeneration. Curr Top Dev Biol. 78:47–126.

Foster BL, Sheen CR, Hatch NE, Liu J, Cory E, Narisawa S, Kiffer-Moreira T, Sah RL, Whyte MP, Somerman MJ, et al. 2015. Periodontal defects in the A116T knock-in murine model of odontohypophosphatasia. J Dent Res. 94(5):706–714.

Foster BL, Soenjaya Y, Nociti FH, Holm E, Zerfas PM, Wimer HF, Holdsworth DW, Aubin JE, Hunter GK, Goldberg HA, et al. 2013. Deficiency in acellular cementum and periodontal attachment in bsp null mice. J Dent Res. 92(2):166–172.

Gasque KC, Foster BL, Kuss P, Yadav MC, Liu J, Kiffer-Moreira T, van Elsas A, Hatch N, Somerman MJ, Millan JL. 2015. Improvement of the skeletal and dental hypophosphatasia phenotype in Alpl(-/-) mice by administration of soluble (non-targeted) chimeric alkaline phosphatase. Bone. 72:137–147.

Houston B, Stewart AJ, Farquharson C. 2004. PHOSPHO1-A novel phosphatase specifically expressed at sites of mineralisation in bone and cartilage. Bone. 34(4):629–637.

Huesa C, Houston D, Kiffer-Moreira T, Yadav MM, Millan JL, Farquharson C. 2015. The functional co-operativity of tissue-nonspecific alkaline phosphatase (TNAP) and PHOSPHO1 during initiation of skeletal mineralization. Biochem Biophys Rep. 4:196–201.

Huesa C, Yadav MC, Finnilä MA, Goodyear SR, Robins SP, Tanner KE, Aspden RM, Millán JL, Farquharson C. 2011. PHOSPHO1 is essential for mechanically competent mineralization and the avoidance of spontaneous fractures. Bone. 48(5):1066–1074.

Javaheri B, Carriero A, Staines KA, Chang YM, Houston DA, Oldknow KJ, Millan JL, Kazeruni BN, Salmon P, Shefelbine S, et al. 2015. Phospho1 deficiency transiently modifies bone architecture yet produces consistent modification in osteocyte differentiation and vascular porosity with ageing. Bone. 81:277–291.

Jono S, McKee MD, Murry CE, Shioi A, Nishizawa Y, Mori K, Morii H, Giachelli CM. 2000. Phosphate regulation of vascular smooth muscle cell calcification. Circ Res. 87(7):E10-17.

Kuss P, Villavicencio-Lorini P, Witte F, Klose J, Albrecht AN, Seemann P, Hecht J, Mundlos S. 2009. Mutant Hoxd13 induces extra digits in a mouse model of synpolydactyly directly and by decreasing retinoic acid synthesis. J Clin Invest. 119(1):146–156.

Macrae VE, Davey MG, McTeir L, Narisawa S, Yadav MC, Millan JL, Farquharson C. 2010. Inhibition of PHOSPHO1 activity results in impaired skeletal mineralization during limb development of the chick. Bone. 46(4):1146–1155.

McKee MD, Yadav MC, Foster BL, Somerman MJ, Farquharson C, Millan JL. 2013. Compounded PHOSPHO1/ALPL deficiencies reduce dentin mineralization. J Dent Res. 92(8):721–727.

Rittling SR, Matsumoto HN, McKee MD, Nanci A, An XR, Novick KE, Kowalski AJ, Noda M, Denhardt DT. 1998. Mice lacking osteopontin show normal development and bone structure but display altered osteoclast formation in vitro. J Bone Miner Res. 13(7):1101–1111.

Roberts S, Narisawa S, Harmey D, Millan JL, Farquharson C. 2007. Functional involvement of PHOSPHO1 in matrix vesicle-mediated skeletal mineralization. J Bone Miner Res. 22(4):617–627.

Rodriguez-Florez N, Garcia-Tunon E, Mukadam Q, Saiz E, Oldknow KJ, Farquharson C, Millan JL, Boyde A, Shefelbine SJ. 2015. An investigation of the mineral in ductile and brittle cortical mouse bone. J Bone Miner Res. 30(5):786–795.

Soenjaya Y, Foster BL, Nociti FH Jr, Ao M, Holdsworth DW, Hunter GK, Somerman MJ, Goldberg HA. 2015. Mechanical forces exacerbate periodontal defects in Bsp-null mice. J Dent Res. 94(9):1276–1285.

Stewart AJ, Roberts SJ, Seawright E, Davey MG, Fleming RH, Farquharson C. 2006. The presence of PHOSPHO1 In matrix vesicles and its developmental expression prior to skeletal mineralization. Bone. 39(5):1000–1007.

Stewart AJ, Schmid R, Blindauer CA, Paisey SJ, Farquharson C. 2003. Comparative modelling of human PHOSPHO1 reveals a new group of phosphatases within the haloacid dehalogenase superfamily. Protein Eng. 16(12):889–895.

Takano Y, Sakai H, Baba O, Terashima T. 2000. Differential involvement of matrix vesicles during the initial and appositional mineralization processes in bone, dentin, and cementum. Bone. 26(4):333–339.

Takano Y, Sakai H, Watanabe E, Ideguchi-Ohma N, Jayawardena CK, Arai K, Asawa Y, Nakano Y, Shuda Y, Sakamoto Y, et al. 2003. Possible role of dentin matrix in region-specific deposition of cellular and acellular extrinsic fibre cementum. J Electron Microsc (Tokyo). 52(6):573–580.

VandenBos T, Bronckers A, Goldberg H, Beertsen W. 1999. Blood circulation as source for osteopontin in acellular extrinsic fiber cementum and other mineralizing tissues. J Dent Res. 78(11):1688–1695.

Yadav MC, Huesa C, Narisawa S, Hoylaerts MF, Moreau A, Farquharson C, Millan JL. 2014. Ablation of osteopontin improves the skeletal phenotype of phospho1 mice. J Bone Miner Res. 29(11):2369–2381.

Yadav MC, Simao AM, Narisawa S, Huesa C, McKee MD, Farquharson C, Millan JL. 2011. Loss of skeletal mineralization by the simultaneous ablation of phospho1 and alkaline phosphatase function: a unified model of the mechanisms of initiation of skeletal calcification. J Bone Miner Res. 26(2):286–297.

Ye L, Zhang S, Ke H, Bonewald L, Feng J. 2008. Periodontal breakdown in the Dmp1 null mouse model of hypophosphatemic rickets. J Dent Res. 87(7):624–629.

Yuan J, Ju E, Yang J, Chen X, Li H. 2014. Different patterns of puberty effect in neural oscillation to negative stimuli: sex differences. Cogn Neurodyn. 8(6):517–524.

Zweifler LE, Patel MK, Nociti FH, Wimer HF, Millán JL, Somerman MJ, Foster BL. 2015. Counter-regulatory phosphatases TNAP and NPP1 temporally regulate tooth root cementogenesis. Int J Oral Sci. 7(1):27–41.